AIMS Mathematics, 11(11): 37954–37975.
DOI: 10.3934/math.20261467
Received: 30 July 2026
Revised: 21 October 2026
Accepted: 27 October 2026
Published: 16 November 2026

https://www.aimspress.com/journal/Math

Research article

Anti-deception attack observer with self-adaptive event triggering for discrete singular networked control systems

Zihan Zhao, Zhihao Wang, Xuetong Zhang, Chenglong Zhu and Guangming Zhuang*

Department of Mathematics and Systems Science, Liaocheng University, Liaocheng, Shandong 252059, China

* **Correspondence:** Email: zgmtsg@126.com.

Abstract: This paper investigates resilient sliding mode regulation with self-adjustable event transmission strategies for discrete-time singular networked plants (DTSNPs) suffering from deception cyberattacks. To counter malicious deception attacks, an integrated observer-aided sliding-mode regulation framework combined with event-based communication protocols is constructed to maintain the operational safety and satisfactory performance of DTSNPs. Using the singular value decomposition technique, novel linear matrix inequality-based sufficient conditions are derived to establish the regularity, causality, and uniform boundedness of the considered singular dynamic system. The elaborately derived sliding mode law further realizes finite-time convergence of all state trajectories toward a tiny bounded region near the system equilibrium point. A singular direct current (DC) motor system serving as an illustrative example verifies the state-estimation, disturbance-suppression, and actuator-attack-mitigation capabilities of the proposed resilient control scheme.

Keywords: discrete-time singular networked plants; deception attacks; observer-based sliding mode; self-adjustable event transmission; linear matrix inequalities
Mathematics Subject Classification: 68T07, 93C57

1. Introduction

Singular dynamic characteristics are widespread in various practical industrial systems, whose state variables evolve at disparate time rates and generate distinct dynamic behaviors. Unlike standard state-space systems that only contain differential or difference equations, singular systems couple dynamic equations with algebraic constraint relations, which can precisely depict the rapid transient variation of system states [1]. Thanks to this unique structural property, singular mathematical frameworks have been extensively adopted to describe a wide range of engineering objects, covering

robot manipulators, flight vehicle dynamics, and industrial chemical reaction systems [2, 3]. Among singular categories, discrete-time singular systems possess more complicated analytical properties in terms of regularity, causality, and global stability relative to normal discrete systems [4]. Such inherent structural complexity raises higher barriers to analyzing and designing stabilizing control strategies, making stability analysis and controller synthesis of discrete singular systems a challenging research topic [5, 6]. So far, fruitful results have been reported for the admissibility analysis and stabilization control of discrete-time singular systems [4–6]. However, most of these studies are carried out under the point-to-point wired communication framework, and rarely involve the communication resource constraints and network security threats in networked deployment scenarios.

Practical discrete-time singular systems usually rely on shared communication networks for signal interaction and data transmission, thus forming discrete-time singular networked plants (DTSNPs) with limited network bandwidth [7–9]. Different from conventional point-to-point wired control systems, DTSNPs feature outstanding advantages in operational flexibility, equipment expansion, and engineering practicability [10–12]. However, the open and shared network transmission environment also brings unprecedented technical difficulties to system control design [13–15]. The researchers [16–18] introduced a series of key research problems including signal sampling scheduling, adaptive event-triggered transmission optimization, and network security defense control. In view of network resource constraints and potential security risks, optimizing data transmission modes, eliminating redundant signal interaction, and improving overall network communication efficiency have become essential and urgent research topics in the field of modern control engineering for DTSNPs [19–21]. To address these issues, event-triggered control has become a mainstream solution, which can effectively reduce communication frequency while preserving control performance. Nevertheless, most existing event-triggered schemes for singular systems adopt fixed triggering thresholds, which are difficult to adapt to dynamically changing operating conditions, leading to either excessive communication resource occupation or degraded control performance [22, 23].

To resolve the communication resource limitation problem of DTSNPs, event-triggered mechanisms (ETMs) have emerged as a promising optimization method in modern control research [24]. This advanced communication scheduling strategy can effectively reduce redundant data interaction during system operation while guaranteeing satisfactory control performance [25–27]. To further enhance the adaptability and transmission efficiency of ETMs in complex operating scenarios, numerous improved strategies have been developed, among which the self-adjustable event transmission scheme has found widespread application [28, 29]. Differing from fixed-threshold triggering strategies, the proposed self-adjustable transmission scheme adopts dynamically adjustable triggering parameters that can update in real time with the variation of system operating states. This adaptive adjustment characteristic significantly reduces invalid data transmission, effectively saves limited network bandwidth resources, and maintains the stable and reliable operation of DTSNPs [30–32]. However, the existing self-adjustable event transmission strategies are mostly developed for regular state-space systems, and their extension to discrete-time singular networked plants still faces theoretical obstacles such as regularity and causality requirements.

Benefiting from open wireless communication channels, DTSNPs realize convenient data interaction, yet they are also exposed to severe cybersecurity threats [33–35]. In complex network industrial scenarios, deception attacks have become one of the most prevalent and destructive malicious network threats [36, 37]. Such hostile attacks mainly target industrial networked control frameworks

and intelligent power systems, where adversaries tamper with real-time transmission data and implant misleading information through covert attack means [38, 39]. These malicious behaviors severely interfere with the normal state judgment and control decision-making of DTSNPs, easily triggering control precision attenuation, system state divergence, and even irreversible operational faults [40, 41]. With the continuous expansion of networked industry, the stealthy and destructive characteristics of deception attacks have become increasingly prominent, posing a critical hidden danger to the stable and safe operation of singular networked control systems, which urgently requires targeted anti-attack control research [42, 43]. Existing anti-deception attack control methods are mainly oriented to conventional networked systems, and there exist very few results concerning singular networked systems. In particular, the cooperative design of event-triggered communication and anti-attack control for DTSNPs remains a challenging open problem [40].

As a robust and advanced control strategy, sliding mode regulation has been widely studied and applied in various industrial control domains due to its superior disturbance rejection and strong parameter robustness [44–46]. Different from conventional linear control methods, this nonlinear control technique forces system state trajectories to converge to a preset sliding manifold through discontinuous control inputs. It can effectively attenuate negative impacts caused by model inaccuracies, external perturbations, and time-varying uncertainties, thereby guaranteeing satisfactory dynamic performance and stable operating accuracy [47–49]. Benefiting from its fast response speed and excellent transient regulation capability, the sliding mode strategy has been successfully implemented in numerous practical scenarios, including robot motion control, vehicle dynamic regulation, and motor driving system optimization, which demonstrates its great application potential in complex and interference-prone industrial environments [50–52]. For further theoretical extensions and practical verifications of singular system control, readers may refer to [53, 54]. Nevertheless, most existing sliding mode control results for singular systems focus on continuous-time models, and seldom consider the joint constraints of networked communication, event-triggered scheduling, and cyber deception attacks. This gap motivates us to develop a resilient sliding mode regulation scheme for DTSNPs under deception attacks with self-adaptive event transmission.

This paper will investigate resilient sliding-mode regulation with self-adjustable event-transmission strategies for DTSNPs suffering from deception cyberattacks. To counter malicious deception attacks, an integrated observer-aided sliding-mode regulation framework combined with event-based communication protocols will be constructed to maintain the operational safety and satisfactory performance of DTSNPs. Using the singular value decomposition (SVD) technique, novel linear matrix inequality (LMI)-based sufficient conditions will be derived to establish the regularity, causality, and uniform boundedness of the considered singular dynamic system. The elaborately derived sliding mode law will further realize finite-time convergence of all state trajectories toward a tiny bounded region near the system equilibrium point. A singular DC motor system will serve as an illustrative example to verify the state-estimation, disturbance-suppression, and actuator-attack-mitigation capabilities of the proposed resilient control scheme.

The main highlights of this work are presented below:

(1) A novel self-adjustable event transmission scheme is developed to reduce bandwidth consumption for DTSNPs. Unlike conventional fixed-threshold triggering strategies, the proposed mechanism uses the latest transmitted data, real-time sampling information, and their averaged features for triggering decisions. It can accurately capture transient system dynamics, maintain

favorable control performance, and greatly cut unnecessary data transmission over the sensor-observer communication channel.

(2) An enhanced observer-based sliding mode regulation strategy is developed to address practical industrial constraints, including unmeasurable system states and network transmission congestion. Leveraging the strong robustness of sliding-mode regulation, the designed controller effectively mitigates adverse effects caused by malicious deception attacks. The proposed scheme improves the system anti-interference capability and attack tolerance, enabling stable and reliable operation of DTSNPs subject to unmeasurable states, network congestion, and deception attacks.

(3) Using the SVD technique, rigorous mathematical conditions are derived to guarantee the regularity, causality, and boundedness of DTSNPs. Combined with the LMI technique, a collaborative observer-based sliding-mode regulation framework integrated with self-adjustable event transmission is constructed for DTSNPs subject to deception attacks. This integrated design eases network transmission load, conserves communication resources, mitigates adverse effects brought by deception attacks, and ultimately improves the overall operational security and stability of DTSNPs.

2. Materials and method

This section designs a self-adaptive event-triggered observer-based sliding mode control for discrete-time singular networked systems against deception attacks, which has three core technical characteristics: (i) a sensor-observer event-triggered mechanism dynamically adjusts thresholds to balance control performance and bandwidth; (ii) an observer recovers unmeasurable states under attacks and event-triggered sampling; and (iii) a robust sliding mode law cooperates with the triggering protocol to attenuate deception attacks and achieve finite-time bounded state convergence.

2.1. System descriptions

The discrete-time singular plant disturbed by deception network attacks is formulated with the following state-space mathematical model:

$$\begin{cases} Ez(k+1) = Fz(k) + N\left(f(k) + v(k)\right), \\ w(k) = Hz(k). \end{cases} \tag{2.1}$$

Here, $v(k) \in \mathbb{R}^m$ is the control command signal, $z(k) \in \mathbb{R}^n$ represents the full state vector of the singular dynamic system, and $w(k) \in \mathbb{R}^p$ signifies the measurable system output. The signal $f(k) \in \mathbb{R}^m$ refers to the maliciously tampered-with data launched by attackers, which behaves as an unknown nonlinear time-varying interference. The matrices satisfy $E \in \mathbb{R}^{n\times n}$, $F \in \mathbb{R}^{n\times n}$, $N \in \mathbb{R}^{n\times m}$, and $H \in \mathbb{R}^{p\times n}$. E is singular ($\text{rank}(E) = r < n$), which can characterize algebraic constraints for singular systems. F, N, and H are constant matrices with matching dimensions, and H has full row rank, $\text{rank}(H) = p$.

2.2. Self-adjustable event transmission scheme

As shown in Figure 1, an event-triggered scheduler between the sensor and observer decides whether sampled outputs are transmitted over shared communication links. To reduce bandwidth usage and improve deception attack robustness, a self-adjustable event transmission scheme is developed.

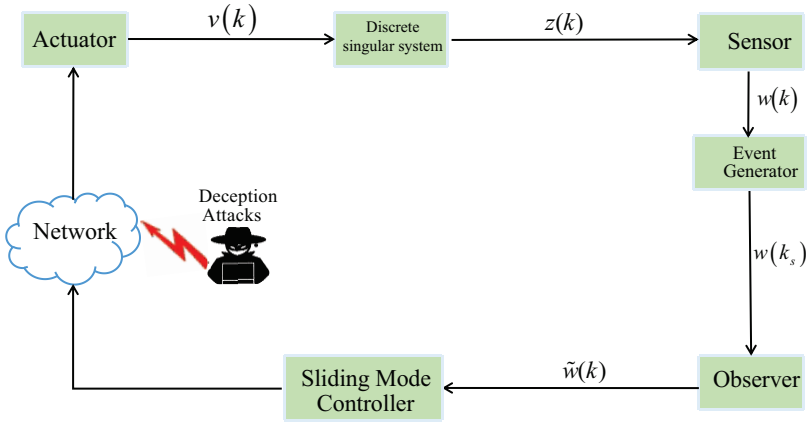


Figure 1. Framework of event-triggered observer sliding mode control for discrete singular networked systems subject to deception attacks.

Let $k \in \mathbb{N}$ denote the current sampling instant and $k_s \in \mathbb{N}$ be the latest release instant at which the sensor output was successfully transmitted. Since only the sensor output signal is transmitted over the network link, define the event-triggered output error as

$$e_w(k, k_s) \triangleq w(k) - w(k_s),$$

i.e., the difference between the measured output at the current sampling instant and the previously transmitted output. Define the average value of the two outputs as $\bar{w}(k, k_s) \triangleq \frac{1}{2}(w(k) + w(k_s))$.

The event-triggered threshold criterion is directly constructed based on the transmitted output error:

$$\left|F^{\frac{1}{2}} e_w(k, k_s)\right|^2 > \delta(k) \left|F^{\frac{1}{2}} \bar{w}(k, k_s)\right|^2, \quad k \in [k_s, k_{s+1}), \tag{2.3}$$

where $\delta(k)$ represents the dynamic threshold. When inequality (2.3) holds, $w(k)$ is transmitted to the observer side and $k_s = k$ is updated accordingly.

Substitute the output equation $w(k) = Hz(k)$ into (2.3). An equivalent triggering condition in the state domain can be derived as

$$\left|F^{\frac{1}{2}} H e_z(k, k_s)\right|^2 > \delta(k) \left|F^{\frac{1}{2}} H \bar{z}(k, k_s)\right|^2,$$

where $e_z(k, k_s) \triangleq z(k) - z(k_s)$ is the state-domain error and $\bar{z}(k, k_s) \triangleq \frac{1}{2}(z(k) + z(k_s))$ denotes the average state.

Remark 2.1. *Zeno behavior is rigorously excluded for the proposed self-adjustable event-triggered scheme. For this discrete-time system with fixed sampling period T, triggering judgments and error updates only occur at $k \in \mathbb{N}$, limiting the triggering frequency to $1/T$. At triggering instant $k = k_s$, $e_s(k_s, k_s) = 0$ leads to $\|F^{1/2} e(k_s, k_s)\| = 0$. Since $\delta(k_s) \geq \delta_0 > 0$ from (2.5), and $w(k)$ is uniformly bounded and nonzero (Theorem 3.1), the right-hand side of (2.3) is strictly positive. Hence, the triggering condition cannot hold immediately after an event, yielding $k_{s+1} - k_s \geq 1$ and a minimum inter-event time T, which ensures the absence of Zeno behavior [7, 9].*

To reconstruct unmeasurable states of singular plants under event-triggered sampling, we construct the state observer:

$$\begin{cases} E\hat{z}(k+1) = F\hat{z}(k) + N(f(k) + v(k)) + L\left(w\left(k_s\right) - \hat{w}(k)\right), \\ \hat{w}(k) = H\hat{z}(k), \end{cases} \tag{2.2}$$

where $\hat{z}(k) \in \mathbb{R}^n$ and $\hat{w}(k) \in \mathbb{R}^p$ denote the estimated state and reconstructed output, respectively, and $L \in \mathbb{R}^{n\times p}$ is the observer gain matrix. The state estimation error is defined as $\tilde{e}_z(k) = z(k) - \hat{z}(k)$.

Remark 2.2. *Distinct from fixed-threshold event-triggered strategies, the proposed scheme employs an arctan-based dynamic threshold $\delta(k)$ synchronized with measurement errors. The threshold adaptively decreases for sharp state variations to guarantee control accuracy and increases in steady state to reduce redundant transmissions. Using real-time and historical data, it captures the transient dynamics of singular systems more precisely, yielding higher communication efficiency with unchanged control performance. Embedded in the sensor-observer channel, the scheduler works with the observer to reconstruct states from intermittent outputs, supporting sliding mode controller design [23, 45].*

2.3. Bounded deception attack

The actuator deception attack signal $f(k)$ is constructed by the attacker only using the intercepted sensor output data transmitted over the network, i.e., it is solely based on the output $w(k_s)$ sent at the last event-triggered instant. The attack energy satisfies the following quadratic constraint:

$$f(k)^T f(k) \leq w(k_s)^T Q^T Q w(k_s), \tag{2.3}$$

where $Q \in \mathbb{R}^{p\times p}$ is a known weighting matrix that characterizes the upper bound of attack strength with respect to the measured output.

Remark 2.3. *Different from state-independent physical disturbances, the state-dependent bounded deception attack $f(k)$ is constructed adversarially using observable system information. Such stealthy attacks mislead control decisions while evading detection, thus being more destructive and difficult to defend against than conventional disturbances [4, 30].*

2.4. Sliding mode regulation design

A sliding mode regulation law is developed to realize stable quasi-sliding motion for the studied discrete-time singular plant. For discrete-time systems, sampling prevents exact sliding, and states oscillate in a bounded neighborhood of the sliding surface, forming quasi-sliding motion [51]. The self-adaptive event-triggered scheme updates the control input and observer correction only at triggering instants, enlarging the boundary layer while saving bandwidth.

The discrete sign($s(k)$) term and event-triggering jointly characterize the closed-loop quasi-sliding mode. The tailored sliding manifold is constructed as

$$s(k) = GE\hat{z}(k) - G(F + NK)\hat{z}(k-1), \tag{2.4}$$

where $K \in \mathbb{R}^{m\times n}$ is the feedback matrix to be determined, and $G \in \mathbb{R}^{m\times n}$ is selected such that GN remains non-singular. The ideal sliding dynamics satisfy $s(k+1) = s(k) = 0$.

When trajectories converge onto the sliding surface, the equivalent control signal is derived as

$$v_{\text{eq}}(k) = (GN)^{-1}GNK\hat{z}(k) - (GN)^{-1}GNf(k) - (GN)^{-1}GL(w(k_s) - \hat{w}(k)), \tag{2.5}$$

where matrix G is chosen to guarantee the invertibility of GN. Substituting $v_{\text{eq}}(k)$ into the singular plant model and defining $\widetilde{G} \triangleq N(GN)^{-1}G$ for brevity, the closed-loop singular dynamics can be rearranged as

$$Ez(k+1) = (F + \widetilde{G}NK)z(k) - \widetilde{G}LHe_w(k, k_s) - (\widetilde{G}NK + \widetilde{G}LH)\tilde{e}_z(k). \tag{2.6}$$

Combining the original plant and observer formulas, we find that the estimation error dynamics satisfy

$$E\tilde{e}(k+1) = (F - LH)\tilde{e}_z(k) - LHe_w(k, k_s). \tag{2.7}$$

By introducing the augmented state vector $z'(k) = \left[z^{\top}(k), \tilde{e}_z^{\top}(k)\right]^{\top}$, the overall augmented singular system can be expressed as

$$\tilde{E}z'(k+1) = \Phi_1 z'(k) + \Phi_2 e_w(k, k_s), \tag{2.8}$$

where

$$\tilde{E} = \begin{bmatrix} E & 0 \\ 0 & E \end{bmatrix}, \quad \Phi_1 = \begin{bmatrix} F + \tilde{G}NK & -\tilde{G}NK - \tilde{G}LH \\ 0 & F - LH \end{bmatrix}, \quad \Phi_2 = \begin{bmatrix} -\tilde{G}LH \\ -LH \end{bmatrix}.$$

Remark 2.4. *For discrete-time singular networked plants under deception attacks, the proposed sliding mode design has three features. First, the sliding manifold (2.7) built from singular matrix E and estimated states accommodates algebraic constraints of singular systems and circumvents full-state measurement difficulty. Second, compatible with aperiodic event-triggered outputs, the robust sliding mode law (Theorem 3.3) compensates estimation errors, event-triggered residuals, and deception attacks via an adaptive robust term, ensuring sliding surface reachability under multiple disturbances. Third, different from continuous-time ideal sliding modes, this design achieves quasi-sliding mode for discrete singular systems: State trajectories converge to a bounded neighborhood of the equilibrium in finite time, consistent with practical discrete networked control behavior [52, 53].*

Lemma 2.1. *Under the event-triggered mechanism (2.3), the deception attack signal satisfies*

$$f(k)^T f(k) \leq \gamma_1 z^T(k) H^T H z(k) + \gamma_2 e_w^T(k, k_s) e_w(k, k_s),$$

where $\gamma_1 = 2\lambda_{\max}(Q^T Q)$, $\gamma_2 = 2\lambda_{\max}(Q^T Q)$, and $e_w(k, k_s) = w(k) - w(k_s)$ denotes the event-triggered output error.

Proof. Substitute $w(k_s) = w(k) - e_w(k, k_s)$ into the attack constraint and expand the quadratic term:

$$w(k_s)^T Q^T Q w(k_s) = (w(k) - e_w(k, k_s))^T Q^T Q (w(k) - e_w(k, k_s)).$$

Applying Young's inequality to bound the cross term yields

$$w(k_s)^T Q^T Q w(k_s) \leq 2w(k)^T Q^T Q w(k) + 2e_w(k, k_s)^T Q^T Q e_w(k, k_s).$$

Substitute the system output equation $w(k) = Hz(k)$. Using the property of the induced matrix norm $w^T Q^T Q w \leq \lambda_{\max}(Q^T Q) w^T w$, the desired result can be obtained immediately.

3. Results

3.1. Summary of main results

This section presents three core theorems for the considered discrete-time singular networked plants under deception attacks and self-adjustable event-triggered communication. Theorem 3.1 provides sufficient conditions ensuring regularity, causality, and uniform boundedness of the augmented closed-loop system. Theorem 3.2 transforms the nonlinear coupled conditions into solvable LMIs for simultaneous computation of observer and sliding-mode controller gains. Theorem 3.3 verifies finite-time quasi-sliding-mode reachability such that system states converge to a bounded neighborhood of equilibrium. These theoretical results will be validated by numerical simulations in the next section.

Theorem 3.1. *The augmented discrete-time singular plant (2.8) is regular, causal, and uniformly bounded, if there exist a symmetric positive definite matrix $P \in \mathbb{R}^{n\times n}$ and matrices U_i $(i = 1, 2, \ldots, 4)$ satisfying the following matrix inequality:*

$$\Xi = \begin{bmatrix} \alpha_{11} & \alpha_{12} \\ * & \alpha_{22} \end{bmatrix} < 0, \tag{3.1}$$

where

$$\alpha_{11} = \begin{bmatrix} \tau_1 & U_1\Phi_2 + \frac{1}{2}\Omega_2 \\ * & \frac{1}{4}\delta\tilde{F} - \tilde{F} \\ * & * \end{bmatrix}, \quad \alpha_{12} = \begin{bmatrix} \tau_2 & \Phi_1^T \\ \Phi_2^T U_4^T & \Phi_2^T \end{bmatrix}, \quad \alpha_{22} = \begin{bmatrix} -U_4 - U_4^T & 0 \\ * & -P^{-1} \end{bmatrix}.$$

$\tau_1 = \Xi_{11} + \Omega_1$, $\tau_2 = -U_1 + (\Phi_1 - E)^T U_4^T + U_5 S^T$, and $S \in \mathbb{R}^{n\times(n-r)}$ is a full-column-rank matrix satisfying $E^T S = 0$. The intermediate matrix is defined as $\tilde{F} = H^T F H$; Ω_1 and Ω_2 denote bounded weighting matrices related to the self-adjustable event transmission scheme, and Φ_1 and Φ_2 are the state and disturbance coupling matrices of the augmented singular system (2.8).

Proof. The proof is split into two segments: regularity and causality analysis, and uniform boundedness verification.

Step 1: Verify regularity and causality of the augmented singular plant (2.8). From the negative definite condition $\Xi < 0$, the sub-block matrix inequality below naturally holds:

$$\Omega = \begin{bmatrix} \Xi_{11} & \Xi_{13} \\ * & \Xi_{33} \end{bmatrix} < 0. \tag{3.2}$$

Left-multiply and right-multiply the above inequality by $[I\ \Phi_1^T]$ and its transpose respectively, which yields a strict negative quadratic constraint on the system matrices.

Since $\tilde{E}$ is singular with $\text{rank}(\tilde{E}) = 2r < 2n$, we introduce two invertible matrices M and N to perform the canonical decomposition of $\tilde{E}$:

$$M\tilde{E}N = \begin{bmatrix} I_{2r} & 0 \\ 0 & 0 \end{bmatrix}, \quad M\Phi_1 N = \begin{bmatrix} \Phi_{11} & \Phi_{12} \\ \Phi_{21} & \Phi_{22} \end{bmatrix},$$

where $\Phi_{11} \in \mathbb{R}^{2r\times 2r}$, $\Phi_{12} \in \mathbb{R}^{2r\times 2(n-r)}$, $\Phi_{21} \in \mathbb{R}^{2(n-r)\times 2r}$, and $\Phi_{22} \in \mathbb{R}^{2(n-r)\times 2(n-r)}$.

Define the transformed matrices:

$$M^{-T}\tilde{S} = \begin{bmatrix} 0 \\ S_1 \end{bmatrix}, \quad N^T U_4 = \begin{bmatrix} U_{41} \\ U_{42} \end{bmatrix},$$

where $S_1 \in \mathbb{R}^{2(n-r)\times 2(n-r)}$ is non-singular due to the full-column-rank property of $\tilde{S}$. Substituting these block forms into the derived quadratic inequality and extracting the bottom-right sub-block related to Φ_{22}, we have

$$U_{52}S_1^T\Phi_{22} + \Phi_{22}^T S_1 U_{52}^T < 0.$$

This inequality directly implies that Φ_{22} is invertible (see [1, Lemma 2.1]). According to the standard definition of regularity and causality for discrete singular systems, the matrix pair $(\tilde{E}, \Phi_1)$ is regular and causal, which satisfies the fundamental well-posedness requirements of discrete singular dynamics.

Step 2: Prove the uniform boundedness of the closed-loop system. Define the state increment vector $\eta(k) \triangleq z'(k+1) - z'(k)$ to characterize the one-step variation of the augmented state $z'(k) = [z^\top(k), \tilde{e}^\top(k)]^\top$. Consider the singular-type Lyapunov functional candidate:

$$V(k) = z'^T(k)\tilde{E}^T P\tilde{E}z'(k) + f(k)^T f(k), \tag{3.3}$$

where the first term accommodates the singular matrix structure of the augmented system, and the second term quantifies the energy bound of deception attacks.

According to Lemma 2.1 (in this paper), the energy of the deception attack can be expressed as quadratic forms of the system state and the event-triggered error. Substituting the attack bound into the Lyapunov increment $\Delta V(k) = V(k+1) - V(k)$ and combining it with the augmented system dynamics $\tilde{E}z'(k+1) = \Phi_1 z'(k) + \Phi_2 e_w(k, k_s)$, we obtain

$$\Delta V(k) = z'^T(k+1)\tilde{E}^T P\tilde{E}z'(k+1) - z'^T(k)\tilde{E}^T P\tilde{E}z'(k) + \Delta f(k),$$

where $\Delta f(k) = f(k+1)^T f(k+1) - f(k)^T f(k)$, which can be upper-bounded by the quadratic forms of the state error and event-triggered error in light of Lemma 2.1 (in this paper),.

Compute the Lyapunov increment $\Delta V(k) = V(k+1) - V(k)$. Substituting the augmented dynamics $\tilde{E}z'(k+1) = \Phi_1 z'(k) + \Phi_2 e_w(k, k_s)$ into the difference function, we obtain

$$\Delta V(k) = z'^T(k+1)\tilde{E}^T P\tilde{E}z'(k+1) - z'^T(k)\tilde{E}^T P\tilde{E}z'(k) + f(k+1)^T f(k+1) - f(k)^T f(k).$$

To handle the coupling terms of state errors and triggered measurement residuals, we introduce two groups of zero-value auxiliary equations for free matrices U_i:

$$2\left[z'^T(k)U_1 + (E\eta(k))^T U_4\right]\left[(\Phi_1 - \tilde{E})z'(k) + \Phi_2 e_w(k, k_s) - E\eta(k)\right] = 0,$$

$$2z'^T(k)U_5\tilde{S}^T E\eta(k) = 0.$$

These identities hold for any matrices U_1, U_4, and U_5, which are introduced as free variables to facilitate the LMI formulation.

Combine the Lyapunov difference with the two zero identities, and then reorganize all quadratic terms into a compact matrix form $\beta^T(k)\Xi'\beta(k)$, where $\beta^T(k) = \left[z'^T(k),\ e_w^T(k,k_s),\ (E\eta(k))^T\right]$; the composite matrix Ξ' is structured as the block negative definite matrix below:

$$\Xi' = \begin{bmatrix} \Xi_{11}+\Xi'_{11} & \Xi_{12} & \Xi_{13} \\ * & \Xi_{22} & \Xi_{23} \\ * & * & \Xi_{33} \end{bmatrix} < 0,$$

with each sub-block defined as

$$\Xi_{11} = -E^TPE + U_1(\Phi_1 - E) + (\Phi_1 - E)^TU_1^T,\ \Xi'_{11} = \Phi_1^TP\Phi_1 + \Omega_1,\ \Xi_{12} = \Phi_1^TP\Phi_2 + U_1\Phi_2 + \frac{1}{2}\Omega_2,$$
$$\Xi_{13} = -U_1 + (\Phi_1 - E)^TU_4^T + U_5S^T,\ \Xi_{22} = \Phi_2^TP\Phi_2 + \frac{1}{4}\delta\tilde{F} - \tilde{F},\ \Xi_{23} = \Phi_2^TU_4^T,\ \Xi_{33} = -U_4 - U_4^T.$$

Since $\Xi' < 0$, there exists a positive scalar $\psi > 0$ such that

$$\Delta V(k) \le -\psi V(k) + 2\bar{Q}. \tag{3.3}$$

This standard exponentially bounded recursive inequality guarantees that all system states remain uniformly bounded for all $k > 0$. The regularity, causality, and boundedness of the augmented plant are all verified, completing the proof of Theorem 3.1.

Theorem 3.1 gives a sufficient stability condition via matrix inequalities, yet it cannot directly solve for gains K and L owing to nonlinear coupling between the singular matrix and gain variables. In the next theorem, congruence transformation and matrix relaxation are adopted to convert the condition into solvable LMIs, enabling simultaneous co-design of the observer and sliding mode controller.

Theorem 3.2. *Consider the discrete-time singular networked plant subject to deception attacks. Given a scalar $\delta_1 > 0$, a known positive scalar q, a full-column-rank matrix $S \in \mathbb{R}^{n\times(n-r)}$ satisfying $E^TS = 0$, and a matrix $G \in \mathbb{R}^{m\times n}$ such that GN is non-singular, if there exist symmetric positive definite matrices $X_1, X_2 \in \mathbb{R}^{n\times n}$, matrices $U_{41}, U_{42} \in \mathbb{R}^{n\times n}$, $U_{51}, U_{52} \in \mathbb{R}^{n\times n}$, $Y \in \mathbb{R}^{m\times n}$, and $Z \in \mathbb{R}^{n\times p}$, such that*

$$\overline{\Xi} = \begin{bmatrix} \overline{\Lambda}_{11} & \overline{\Lambda}_{12} \\ * & \overline{\Lambda}_{22} \end{bmatrix} < 0, \tag{3.4}$$

where

$$\overline{\Lambda}_{11} = \begin{bmatrix} \bar{\theta}_{11} & \bar{\theta}_{12} \\ * & \bar{\theta}_{22} \end{bmatrix},\quad \overline{\Lambda}_{12} = \begin{bmatrix} \bar{\Lambda}_1 \\ \bar{\Lambda}_2 \end{bmatrix},\quad \overline{\Lambda}_{22} = \begin{bmatrix} -X_1 & 0 \\ * & -X_2 \end{bmatrix},$$
$$\bar{\theta}_{11} = \begin{bmatrix} \bar{\alpha}_{11} & \bar{\alpha}_{12} & \bar{\alpha}_{13} \\ * & \bar{\alpha}_{22} & \bar{\alpha}_{23} \\ * & * & \bar{\alpha}_{33} \end{bmatrix},\quad \bar{\theta}_{12} = \begin{bmatrix} \bar{\beta}_{11} & 0 \\ \bar{\beta}_{21} & \bar{\beta}_{22} \\ \bar{\beta}_{31} & \bar{\beta}_{32} \end{bmatrix},\quad \bar{\theta}_{22} = \begin{bmatrix} \bar{\gamma}_{11} & 0 \\ 0 & \bar{\gamma}_{22} \end{bmatrix},$$
$$\bar{\Lambda}_1 = \begin{bmatrix} \tau_1 & 0 \\ \tau_2 & \tau_3 \end{bmatrix},\quad \bar{\Lambda}_2 = \begin{bmatrix} -Z^T\tilde{G}^T & -Z^T \\ 0 & 0 \\ 0 & 0 \end{bmatrix},$$

with each block element defined as

$$\begin{aligned}
&\bar{\alpha}_{11} = -qE^T - qE + q^2X_1 + FX_1 + \tilde{G}NY + X_1F^T + Y^TN^T\tilde{G}^T + \delta_1\tilde{F}, \quad \bar{\alpha}_{13} = -\tilde{G}Z + \tfrac{1}{2}\delta_1\tilde{F},\\
&\bar{\alpha}_{22} = FX_2 - Z - EX_2 + X_2F^T - Z^T - X_2E^T - qE^T - qE + q^2X_2,\\
&\bar{\alpha}_{23} = -Z, \quad \bar{\alpha}_{33} = \tfrac{1}{4}\delta_1\tilde{F} - \tilde{F}, \quad \bar{\alpha}_{12} = -\tilde{G}NY - \tilde{G}Z,\\
&\bar{\beta}_{11} = -U_{41}^T + F^T - E^T + U_{51}S^T, \quad \bar{\beta}_{21} = -Y^TN^T\tilde{G}^T - Z^T\tilde{G}^T,\\
&\bar{\beta}_{22} = -U_{42}^T + F^T - Z - E^T + U_{52}S^T, \quad \bar{\beta}_{31} = -Z^T\tilde{G}^T, \quad \bar{\beta}_{32} = -Z^T,\\
&\bar{\gamma}_{11} = -U_{41} - U_{41}^T, \quad \bar{\gamma}_{22} = -U_{42} - U_{42}^T,\\
&\tau_1 = X_1F^TE^T + Y^TN^T\tilde{G}^TE^T, \quad \tau_2 = -Y^TN^T\tilde{G}^TE^T - Z^T\tilde{G}^TE^T, \quad \tau_3 = X_2F^TE^T - Z^TE^T,
\end{aligned}$$

and $\tilde{G} \triangleq N(GN)^{-1}G$, $\tilde{F} = H^TFH$, *then there exist a sliding mode controller gain* K *and an observer gain* L *such that the closed-loop augmented system is regular, causal, and uniformly bounded. The gains are reconstructed by*

$$K = YX_1^{-1}, \quad L = ZH^{-1}. \tag{3.5}$$

Proof. Let the block-diagonal matrices matching the augmented system be

$$P = \mathrm{diag}\{P_1, P_2\}, \quad U_4 = \mathrm{diag}\{U_{41}, U_{42}\}, \quad U_5 = \mathrm{diag}\{U_{51}, U_{52}\},$$

where P_1 and P_2 correspond to the original plant state and the estimation error state, respectively.

From Theorem 3.1, the closed-loop system is regular, causal, and uniformly bounded if and only if $\Xi < 0$. Define the invertible transformation matrices

$$X_1 = P_1^{-1}, \quad X_2 = P_2^{-1},$$

and introduce new decision variables

$$Y = KX_1, \quad Z = LHX_2.$$

Pre- and post-multiplying $\Xi < 0$ by $\mathrm{diag}\{X_1, X_2, I, U_{41}^{-T}, U_{42}^{-T}, I, I\}$ and its transpose respectively, the inequality sign remains unchanged by the property of congruent transformation.

Substituting $P_1X_1 = I$, $P_2X_2 = I$, $KX_1 = Y$, and $LHX_2 = Z$ into the inequality, expanding and rearranging all block elements yield the equivalent LMI condition $\overline{\Xi} < 0$ in the theorem statement.

Since the congruent transformation is invertible, $\Xi < 0$ is equivalent to $\overline{\Xi} < 0$. When the LMI is feasible, the controller and observer gains can be uniquely reconstructed by $K = YX_1^{-1}$ and $L = ZH^{-1}$. This completes the proof.

The above two theorems guarantee the regularity, causality, and uniform boundedness of the closed-loop singular system. In the following theorem, we further prove the finite-time convergence property of the sliding mode motion, i.e., the quasi-sliding mode behavior for the discrete-time singular plant under deception attacks and event-triggered communication.

Remark 3.1. *All block matrices in the above LMI conditions are explicitly defined with known system matrices and decision variables. The LMI can be directly solved by standard numerical tools such as the MATLAB LMI Control Toolbox, and the controller and observer gains can be uniquely extracted from the feasible solution, which guarantees the reproducibility of the proposed design method.*

Theorem 3.3. *For the discrete-time singular plant (2.8) disturbed by deception attacks, all state trajectories can be driven into a bounded compact region near the equilibrium within finite time and stay inside this region persistently, under the proposed sliding mode regulation law below. This theorem theoretically characterizes the quasi-sliding mode property of the closed-loop system: The system state does not converge to the equilibrium point exactly in finite time, but enters a bounded compact region near the equilibrium and remains bounded thereafter, which is the standard definition of quasi-sliding mode in discrete-time sliding mode control. The feedback gain matrix K in (3.9) is solved from Theorem 3.2, and G is selected such that GN is non-singular.*

$$v(k) = K\hat{z}(k) - \rho(k)\, sign(s(k)), \tag{3.6}$$

where

$$\rho(k) = \rho + \left\|(GN)^{-1}GLH\right\| \left\|\tilde{e}(k)\right\| + \left\|(GN)^{-1}GLH\right\| \left\|e(k, k_s)\right\| + \left\|f(k)\right\|. \tag{3.7}$$

Proof. Select the sliding-mode Lyapunov candidate:

$$V_2(k) = \frac{1}{2} s^T(k)(GN)^{-1}s(k). \tag{3.8}$$

Compute the difference $\Delta V_2(k) = V_2(k+1) - V_2(k)$ and substitute the sliding manifold dynamics and state observer model. After norm-based inequality scaling and simplification, we arrive at

$$\Delta V_2(k) \leq -\rho\|s(k)\| + \frac{1}{2}\Delta s^T(k)(GN)^{-1}\Delta s(k). \tag{3.9}$$

Choosing a sufficiently large positive scalar ρ guarantees $\Delta V_2(k) < 0$ when $s(k)$ lies outside a bounded neighborhood of the origin. Since the increment term $\Delta s(k)$ remains uniformly bounded, all system trajectories converge to a small bounded region around the equilibrium in finite time, which finishes the proof.

4. Simulation

A practical singular plant example, i.e., a DC motor electromechanical system in Figure 2 [54], is adopted to verify the validity of the proposed event-triggered sliding mode observer control strategy against deception attacks.

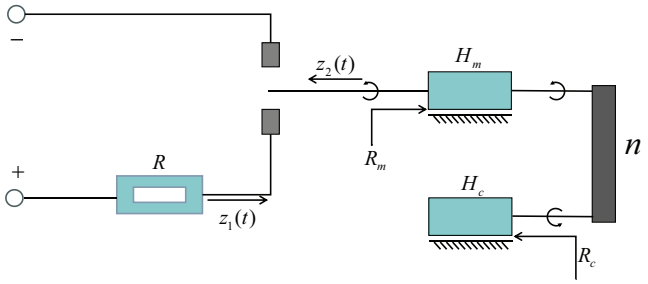


Figure 2. Block diagram of a DC motor singular system.

The DC motor system has coupled electrical and mechanical dynamics, which naturally form a continuous singular system with algebraic constraints between armature current and shaft angular velocity. DC motors are widely used in industrial transmission, robotics, and intelligent manufacturing. In networked control frameworks, actuator channels on shared networks face cyber deception attacks. Such false data injection (FDI) attacks corrupt observer state estimation, trigger steady-state speed errors, and may lead to armature overcurrent and equipment damage. Thus, anti-deception state observer design is essential to maintain safe operation of networked DC motor systems. Define state variables $\xi_1(t) = w(t)$ and $\xi_2(t) = j(t)$. The continuous-time dynamic model is written as

$$\begin{cases} \dot{w}(t) = -\dfrac{R}{H}w(t) + \dfrac{\Theta}{H}j(t), \\ q(t) = \Theta_a w(t) + r\,j(t), \end{cases} \tag{4.1}$$

where composite damping and inertia coefficients satisfy $R = R_m + \dfrac{R_c}{n^2}$ and $H = H_m + \dfrac{H_c}{n^2}$. We discretize the continuous model with fixed sampling period $T = 0.2$ s under the deception attack signal $f(k)$, yielding the discrete singular form

$$Ez(k+1) = Fz(k) + N(v(k) + f(k)), \tag{4.2}$$

with singular matrix

$$E = \begin{bmatrix} 0 & 1 \\ 0 & 0 \end{bmatrix},$$

state matrix F, input matrix N, measurement output matrix H, sliding design matrix $G = \begin{bmatrix} 2 & 2.1 \end{bmatrix}$, and full-column-rank matrix $S = \begin{bmatrix} 0 \\ 1 \end{bmatrix}$ satisfying $E^T S = 0$. The stealthy deception attack signal follows $f(k+1) = f(k) + \epsilon \sin(\omega k)$ with initial condition $f(0) = 0.01\sin(\|e_w(k, k_s)\|)$, where $\epsilon = 0.1$ and $\omega = 0.5$.

System physical parameters are assigned as $R_m = 1.5$, $R_c = 50$, $H_m = 2.5\,\text{kg·m}$, $H_c = 50\,\text{kg·m}$, armature resistance $r = 2\,\Omega$, torque constant $\Theta = 0.4\,\text{Nm/A}$, and back-electromotive force constant $\Theta_a = 0.5\,\text{Vs/rad}$. The self-adjustable event-triggered thresholds $\delta_0 = 0.05$ and $\delta_1 = 0.46$ trade off communication efficiency and control performance. Larger δ_1 lowers transmission frequency yet degrades accuracy; smaller δ_0 enhances precision but raises network burden. Matrix $D = \begin{bmatrix} 0.5 & -0.07 \\ 0.03 & 0.1 \end{bmatrix}$ adjusts the adaptive threshold's convergence rate. Matrix $G = [2 \quad 2.1]$ ensures GN non-singularity and sliding mode reachability. Q is tuned via maximum attack amplitude to meet (2.2). Typical initial deviations verify closed-loop transient performance. The initial state of the DC motor system is chosen as $z(0) = [-0.15,\ 0.6]^\top$, and the initial observer state is set to $\hat{z}(0) = [0.15,\ 0.3]^\top$.

4.1. Comparative methods and evaluation indexes

To verify the merits of the proposed self-adjustable event-triggered sliding mode observer control (SAET-SMO), two benchmark schemes are compared under identical deception attacks and initial conditions:

(1) Fixed-threshold event-triggered SMO (FTET-SMO): It shares the same observer and sliding mode controller but uses a fixed threshold $\delta = 0.25$ (the average of δ_0 and δ_1), to validate the advantage of adaptive thresholds.
(2) Time-triggered SMO (TT-SMO): Sensor data are transmitted at each sampling instant without event triggering, acting as the upper bound of control accuracy to quantify performance degradation brought by event-triggered communication.

All three approaches use identical observer and sliding mode gains obtained from Theorem 3.2. Three metrics are adopted for quantitative evaluation: total data transmissions (network occupancy), state estimation RMSE (observation precision), and steady-state bound of sliding surface $s(k)$ (anti-attack control performance).

By solving the linear matrix inequality constraints proposed in Theorem 3.2, we obtain the feasible Lyapunov matrix P, sliding mode feedback gain K, and observer gain matrix L simultaneously:

$$K = \begin{bmatrix} -7.3588 & -17.9678 \end{bmatrix}, \quad L = \begin{bmatrix} -0.0350 & -0.0679 \\ -0.8341 & -0.6788 \end{bmatrix}, \quad F = \begin{bmatrix} 1.0191 & 0.0029 \\ 0.0029 & 0.9559 \end{bmatrix}.$$

The simulation results for the DC motor singular system are shown in Figures 3–10. Figures 3 and 4 plot the 3D trajectories of the actual state $z(k)$ and reconstructed state $\hat{z}(k)$, illustrating state evolution under deception attacks. The time-domain responses of $z_1(k)$ and $z_2(k)$ and their estimates $\hat{z}_1(k)$ and $\hat{z}_2(k)$ are given in Figures 5 and 6, confirming accurate state tracking by the proposed observer.

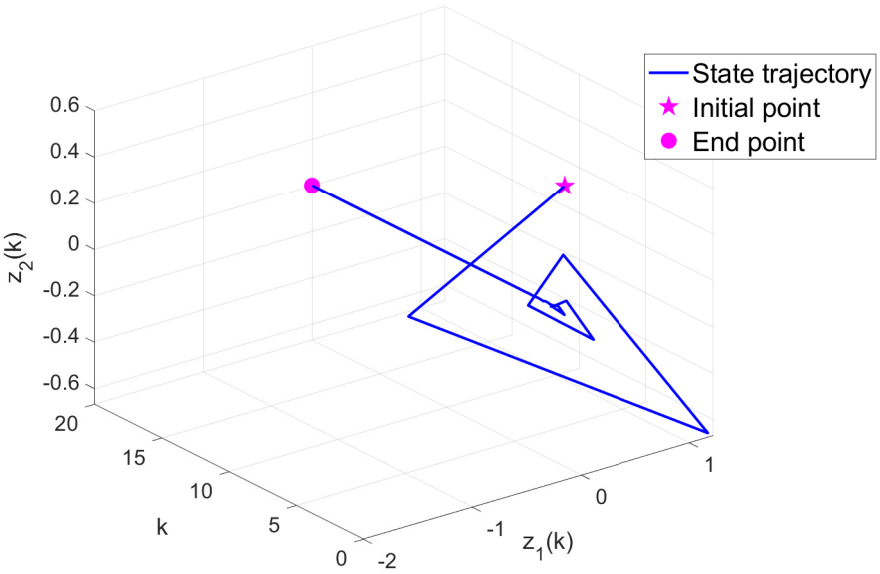


Figure 3. 3D trajectory of system state $z(k)$.

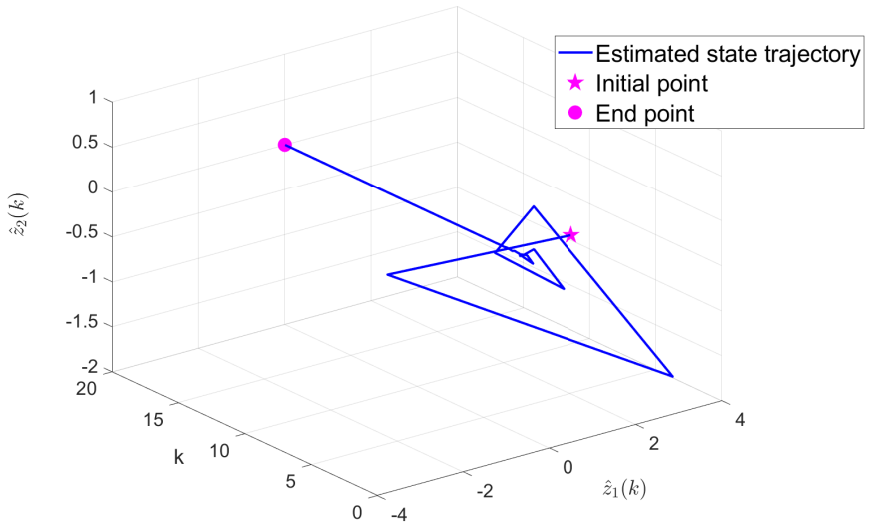


Figure 4. 3D trajectory of estimated state $\hat{z}(k)$.

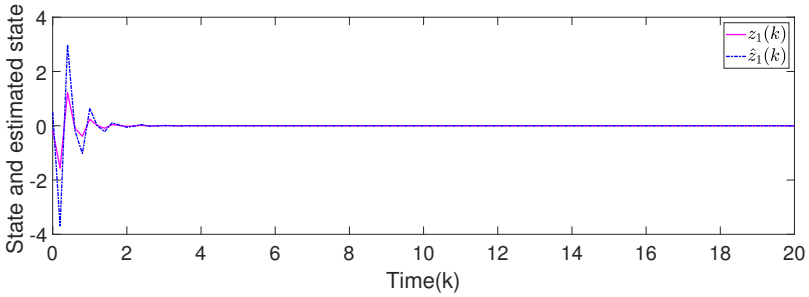


Figure 5. Curves of $z_1(k)$ and its estimate $\hat{z}_1(k)$.

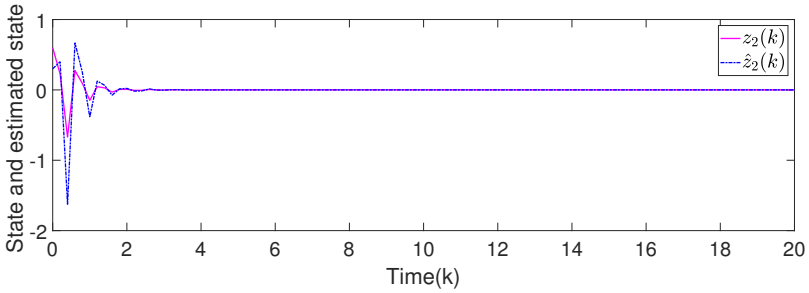


Figure 6. Curves of $z_2(k)$ and its estimate $\hat{z}_2(k)$.

Figure 7 presents the state estimation errors $\tilde{e}_1(k)$ and $\tilde{e}_2(k)$, which converge rapidly to zero and validate the favorable observation performance. The sliding-mode control input $v(k)$ in Figure 8 remains bounded during the simulation. Figure 9 demonstrates that the sliding surface $s(k)$ converges quickly to the origin and stays near zero at all sampling instants, confirming that quasi-sliding motion is preserved under deception attacks. Collectively, these results verify the effectiveness and superiority of the integrated event-triggered adaptive sliding-mode observer control scheme.

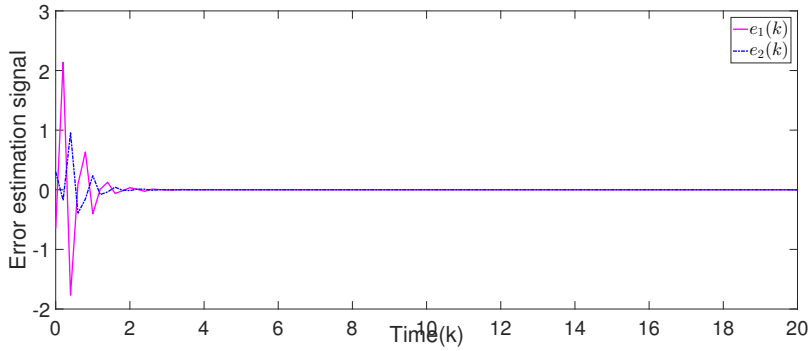


Figure 7. State estimation errors $e_1(k)$ and $e_2(k)$.

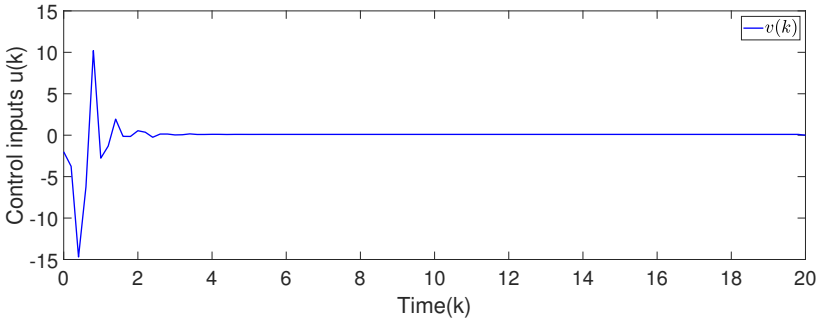


Figure 8. Response curve of control input $v(k)$.

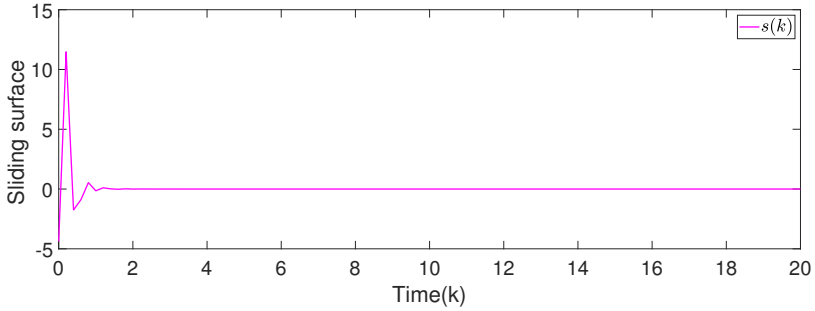


Figure 9. Response curve of sliding surface $s(k)$.

Table 1 compares the static event-triggered mechanism (SETM) and proposed self-adjustable triggering strategy using three metrics: transmitted packet count, mean event release interval, and bandwidth occupancy ratio. Figures 10 and 11 show the SETM and adaptive event-triggered mechanism (AETM) triggering instants and release intervals, respectively. The AETM reduces packet transmissions and bandwidth usage while extending the average release interval, achieving higher communication-resource efficiency than the SETM.

Table 1. Numerical comparison of different ETMs.

	Transmitted packet counts	Bandwidth occupancy ratios	Average release intervals
Static ETM	49	49%	0.408
AETM (in this paper)	43	43%	0.465

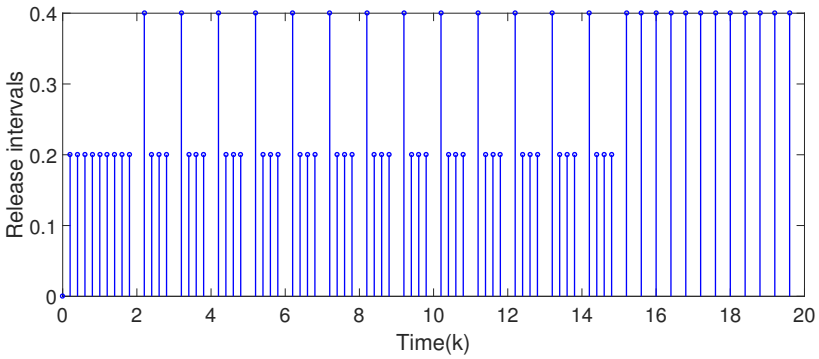


Figure 10. Event-triggered release instants and intervals.

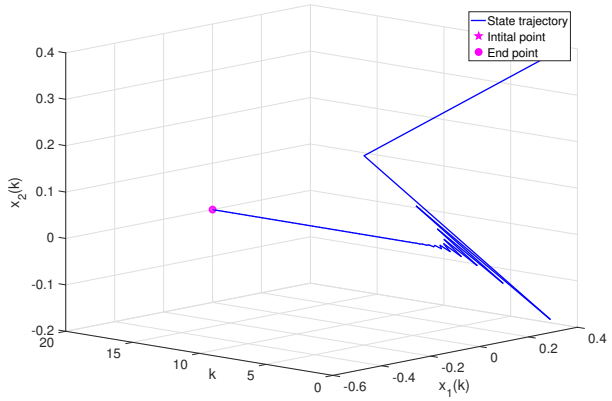


Figure 11. Static time-triggered release instants and intervals.

5. Conclusions

This paper has investigated resilient sliding mode regulation with self-adjustable event-transmission strategies for DTSNPs suffering from deception cyberattacks. To counter malicious deception attacks, an integrated observer-aided sliding-mode regulation framework combined with event-based communication protocols has been constructed to maintain the operational safety and satisfactory performance of DTSNPs. Using the SVD technique, novel LMI-based sufficient conditions have been derived to establish the regularity, causality, and uniform boundedness of the considered singular dynamic system. The elaborately derived sliding mode law has further realized finite-time

convergence of all state trajectories toward a tiny bounded region near the system equilibrium point. A singular DC motor system has served as an illustrative example to verify the state-estimation, disturbance-suppression, and actuator-attack-mitigation capabilities of the proposed resilient control scheme.

Author contributions

Zihan Zhao: Conceptualization, Formal analysis, Writing–original draft; Zhihao Wang: Software, Methodology, Writing–review and editing; Xuetong Zhang: Formal analysis; Chenglong Zhu: Writing–review and editing; Guangming Zhuang: Validation, Visualization. All authors have approved the final manuscript for publication.

Use of Generative-AI tools declaration

The authors declare they have not used Artificial Intelligence (AI) tools in the creation of this article.

Acknowledgments

This work was partly supported by the National Natural Science Foundation of China under Grants 62173174 and 61773191; the Shandong Provincial Natural Science Foundation under Grants ZR2024MF081 and ZR2023QF105; the Postgraduate Education Quality Improvement Plan Project of Liaocheng University under Grant LCUJYZD2501; the Graduate Education High-Quality Curriculum Construction Project for Shandong Province-Introduction to Systems Science under Grant SDYKC2024168.

Conflict of interest

The authors declare that they have no conflicts of interest.

References

1. P. Li, G. R. Duan, B. Zhang, L. M. Wang, Y. Z. Wang, Output position control of two-mass systems based on fully actuated system and singular perturbation approaches, *IEEE/ASME Trans. Mech.*, **31** (2026), 1022–1033. https://doi.org/10.1109/TMECH.2025.3602374
2. T. Saravanakumar, A. Stephen, X. S. Bai, Q. X. Zhu, T. W. Huang, New results on memory sampled-data control design for IT2 fuzzy singular systems with external disturbance, *IEEE Trans. Cybern.*, **56** (2026), 788–801. https://doi.org/10.1109/TCYB.2025.3607281
3. H. Liu, Z. X. Huang, S. Y. Xu, B. Niu, Z. A. Wei, Encrypted zonotopic set-based estimation for cyber-physical systems, *IEEE Trans. Autom. Control*, **71** (2026), 4834–4841. https://doi.org/10.1109/TAC.2026.3662529
4. Z. Lian, P. Shi, C. P. Lim, M. Saif, M. Chen, Designing optimal stealthy false data injection attacks in cyber-physical systems: leveraging historical data and Kullback-Leibler divergence constraints, *IEEE Trans. Autom. Control*, **71** (2026), 2316–2329. https://doi.org/10.1109/TAC.2025.3627271

5. G. L. Chen, J. W. Xia, G. M. Zhuang, J. S. Zhao, Improved delay-dependent stabilization for a class of networked control systems with nonlinear perturbations and two delay components, *Appl. Math. Comput.*, **316** (2018), 1–17. https://doi.org/10.1016/j.amc.2017.07.072
6. T. Yang, G. L. Chen, J. W. Xia, Z. Wang, Q. Sun, Robust H_∞ filtering for polytopic uncertain stochastic systems under quantized sampled outputs, *Appl. Math. Comput.*, **347** (2019), 688–701. https://doi.org/10.1016/j.amc.2018.11.035
7. L. F. Qiu, J. S. Zhao, Adaptive designated-time fuzzy event-triggered tracking of constrained nonlinear systems and its applications in robotic systems, *AIMS Math.*, **11** (2026), 15691–15715. https://doi.org/10.3934/math.2026645
8. F. Amato, L. Y. Qiu, M. Tanveer, S. Cuomo, D. Annunziata, F. Giampaolo, et al., Towards one-shot federated learning: advances, challenges, and future directions, *Neurocomputing*, **664** (2026), 132088. https://doi.org/10.1016/j.neucom.2025.132088
9. X. Wang, G. M. Zhuang, G. L. Chen, Q. Ma, J. W. Lu, Asynchronous mixed H_∞ and passive control for fuzzy singular delayed Markovian jump system via hidden Markovian model mechanism, *Appl. Math. Comput.*, **429** (2022), 127253. https://doi.org/10.1016/j.amc.2022.127253
10. Y. F. Chen, J. W. Xia, J. Zhang, J. H. Park, Q. Ma, Adaptive event-triggered resilient formation collision avoidance control for high-order nonlinear multiagent systems under DoS attacks, *IEEE Trans. Reliab.*, **75** (2026), 3293–3304. https://doi.org/10.1109/TR.2026.3730000
11. K. J. Fan, G. C. Pang, X. Y. Chen, J. D. Cao, J. L. Qiu, Fault-tolerant control of multi-agent systems using a Fourier series observer under DoS attacks and periodic intermittent faults, *Syst. Control Lett.*, **211** (2026), 106397. https://doi.org/10.1016/j.sysconle.2026.106397
12. Y. J. Pang, G. M. Zhuang, J. W. Xia, X. P. Xie, H_∞ security control for singular jump systems with actuator faults and DoS attacks under switching-like adaptive trigger and application to OCCP, *IEEE Trans. Autom. Sci. Eng.*, **22** (2025), 7955–7966. https://doi.org/10.1109/TASE.2024.3475374
13. Y. Gao, W. Sun, S. F. Su, Prescribed-time adaptive output feedback tracking control for nonlinear systems with quantized input, *Appl. Math. Comput.*, **463** (2024), 128370. https://doi.org/10.1016/j.amc.2023.128370
14. Z. H. Wang, X. T. Zhang, Z. H. Zhao, G. M. Zhuang, Observer-based neural integral sliding mode control for singular Markovian jump systems against actuator spoofing attacks, *AIMS Math.*, **11** (2026), 30280–30303. https://doi.org/10.3934/math.20261200
15. M. J. Hao, G. M. Zhuang, G. Z. Cui, J. W. Xia, Observer-based dynamic event-triggered finite-time switching control for networked discrete implicit DC circuit systems under aperiodic DoS attacks, *IEEE Trans. Autom. Sci. Eng.*, **22** (2025), 22925–22937. https://doi.org/10.1109/TASE.2025.3624969
16. X. Y. Liang, J. W. Xia, G. L. Chen, H. S. Zhang, Z. Wang, Dissipativity-based sampled-data control for fuzzy Markovian jump systems, *Appl. Math. Comput.*, **361** (2019), 552–564. https://doi.org/10.1016/j.amc.2019.05.038
17. Y. L. Deng, H. S. Zhang, Y. Z. Dai, Y. Li, Interval stability/stabilization for linear stochastic switched systems with time-varying delay, *Appl. Math. Comput.*, **428** (2022), 127201. https://doi.org/10.1016/j.amc.2022.127201

18. Y. Q. Lin, G. M. Zhuang, W. Sun, J. S. Zhao, Y. M. Chu, Resilient H_∞ dynamic output feedback controller design for USJSs with time-varying delays, *Appl. Math. Comput.*, **395** (2021), 125875. https://doi.org/10.1016/j.amc.2020.125875

19. G. L. Chen, L. Y. Wang, T. Yang, J. W. Xia, J. H. Park, Differentially private mean-square output consensus for heterogeneous multiagent systems: an asynchronous sampled-data interactions scheme, *IEEE Trans. Inf. Forensics Secur.*, **20** (2025), 10189–10202. https://doi.org/10.1109/TIFS.2025.3613051

20. G. L. Chen, M. Y. Tang, T. Yang, J. W. Xia, J. H. Park, Large delay-dependent nonuniform sampling load frequency control: a novel discrete-time feedback interconnection model approach, *IEEE Trans. Control Syst. Technol.*, **34** (2026), 2781–2793. https://doi.org/10.1109/TCST.2026.3714907

21. T. Binazadeh, E. Jafari, Synchronization of chaotic fractional-order systems with input saturation and non-vanishing perturbations: ultimate boundedness analysis and transient behavior improvement, *Int. J. Dyn. Control*, **13** (2025), 134. https://doi.org/10.1007/s40435-025-01633-6

22. Y. Li, H. S. Zhang, T. T. Zhang, H. Geng, Interval stability/stabilization and H_∞ feedback control for linear impulsive stochastic systems, *Appl. Math. Comput.*, **437** (2023), 127552. https://doi.org/10.1016/j.amc.2022.127552

23. J. W. Xia, H. R. Yue, J. Zhang, J. H. Park, Fully distributed optimization algorithm for nonlinear multiagent systems under stochastic event-triggered mechanism, *IEEE Trans. Ind. Inform.*, **21** (2025), 8248–8257. https://doi.org/10.1109/TII.2025.3586059

24. Y. Liu, G. C. Pang, J. L. Qiu, X. Y. Chen, J. D. Cao, Fault-tolerant control for output regulation in multi-agent systems based on prescribed-time observers, *IEEE Trans. Signal Inf. Process. Netw.*, **10** (2024), 729–739. https://doi.org/10.1109/TSIPN.2024.3458789

25. G. L. Chen, G. X. Du, J. W. Xia, X. P. Xie, Z. C. Wang, Aperiodic sampled-data H_∞ control of vehicle active suspension system: an uncertain discrete-time model approach, *IEEE Trans. Ind. Inform.*, **20** (2024), 6739–6750. https://doi.org/10.1109/TII.2024.3353856

26. H. S. Zhang, G. M. Zhuang, W. Sun, Y. M. Li, J. W. Lu, *pth* moment asymptotic interval stability and stabilization of linear stochastic systems via generalized $\mathscr{H}$-representation, *Appl. Math. Comput.*, **386** (2020), 125520. https://doi.org/10.1016/j.amc.2020.125520

27. G. L. Chen, X. R. Liu, X. Q. Ren, J. W. Xia, J. H. Park, Asynchronous-based countermeasure for stealthy attack on aperiodic sampled-data control systems, *IEEE Trans. Autom. Control*, **70** (2025), 6159–6166. https://doi.org/10.1109/TAC.2025.3552745

28. X. Q. Wu, W. Sun, Adaptive fault tolerant optimal control for high-order fully actuated system and its application in spacecraft attitude tracking using reinforcement learning, *Appl. Math. Comput.*, **512** (2026), 129774. https://doi.org/10.1016/j.amc.2025.129774

29. Y. F. Wu, G. M. Zhuang, M. M. Jiang, Y. Q. Wang, H_∞ adaptive ETF control for degenerate jump systems under actuator faults and impulsive deception attacks with application to DCMIP device, *Appl. Math. Comput.*, **489** (2025), 129158. https://doi.org/10.1016/j.amc.2024.129158

30. M. Q. Xing, Y. Q. Wang, G. M. Zhuang, F. Chen, Event-based asynchronous and resilient filtering for singular Markov jump LPV systems against deception attacks, *Appl. Math. Comput.*, **403** (2021), 126176. https://doi.org/10.1016/j.amc.2021.126176

31. R. Shang, W. Sun, Y. G. Sun, Preassigned finite-time load frequency control of power systems with gain learning and deferred prescribed performance, *IEEE Trans. Consum. Electron.*, 2026. https://doi.org/10.1109/TCE.2026.3730422

32. G. L. Chen, C. C. Fan, J. Sun, J. W. Xia, Mean square exponential stability analysis for Itô stochastic systems with aperiodic sampling and multiple time-delays, *IEEE Trans. Autom. Control*, **67** (2022), 2473–2480. https://doi.org/10.1109/TAC.2021.3074848

33. C. L. Zhu, X. L. Ma, W. P. Ding, W. Pedrycz, J. M. Zhan, Long-term prediction model for fuzzy granular time series based on trend filter decomposition and ensemble learning, *IEEE Trans. Cybern.*, **55** (2025), 4514–4527. https://doi.org/10.1109/TCYB.2025.3582771

34. W. J. Yang, J. W. Xia, M. Yu, N. Zhang, Decentralized adaptive funnel control of uncertain large-scale interconnected nonlinear system, *Appl. Math. Comput.*, **441** (2023), 127694. https://doi.org/10.1016/j.amc.2022.127694

35. C. L. Zhu, X. L. Ma, P. D'Urso, Y. H. Qian, W. P. Ding, J. M. Zhan, Long-term multivariate time-series forecasting model based on Gaussian fuzzy information granules, *IEEE Trans. Fuzzy Syst.*, **32** (2024), 6424–6438. https://doi.org/10.1109/TFUZZ.2024.3449769

36. F. Basile, G. De Tommasi, S. Dubbioso, F. Fiorenza, A sequence-based approach for the verification of current-state opacity in bounded discrete event systems, *IEEE Trans. Autom. Control*, **71** (2026), 4340–4354. https://doi.org/10.1109/TAC.2026.3653378

37. J. S. Zhao, L. F. Qiu, X. P. Xie, Z. Y. Sun, Finite-time stabilization of stochastic nonlinear systems and its applications in ship maneuvering systems, *IEEE Trans. Fuzzy Syst.*, **32** (2024), 1023–1035. https://doi.org/10.1109/TFUZZ.2023.3317177

38. H. S. Zhang, Y. Z. Dai, C. L. Zhu, Region stability analysis and precise tracking control of linear stochastic systems, *Appl. Math. Comput.*, **465** (2024), 128402. https://doi.org/10.1016/j.amc.2023.128402

39. J. S. Zhao, Y. X. Yuan, Z. Y. Sun, X. P. Xie, Applications to the dynamics of the suspension system of fast finite time stability in probability of p-norm stochastic nonlinear systems, *Appl. Math. Comput.*, **457** (2023), 128221. https://doi.org/10.1016/j.amc.2023.128221

40. A. R. Wu, H. S. Zhang, J. W. Xia, Interval stabilization for switched stochastic positive systems: a state-dependent switching scheme with convergence rate constraint, *IEEE Trans. Consum. Electron.*, **72** (2026), 3456–3466. https://doi.org/10.1109/TCE.2026.3683018

41. M. Q. Cheng, J. S. Zhao, X. P. Xie, Z. Y. Sun, A novel finite-time stability criteria and controller design for nonlinear impulsive systems, *Appl. Math. Comput.*, **479** (2024), 128876. https://doi.org/10.1016/j.amc.2024.128876

42. D. X. Ren, G. C. Pang, X. J. Mou, X. Y. Chen, J. L. Qiu, J. D. Cao, Simultaneous fault-tolerant consensus control and disturbance suppression for multi-agent systems with polynomial form fault under switching topology, *Syst. Control Lett.*, **193** (2024), 105946. https://doi.org/10.1016/j.sysconle.2024.105946

43. Y. Q. Liu, G. M. Zhuang, J. S. Zhao, J. W. Lu, Z. K. Wang, H_∞ admissibilization for time-varying delayed nonlinear singular impulsive jump systems based on memory state-feedback control, *Appl. Math. Comput.*, **447** (2023), 127921. https://doi.org/10.1016/j.amc.2023.127921

44. X. R. Li, H. S. Zhang, S. F. Su, W. Sun, Control performance orientated region stabilization and H_∞ control of discrete stochastic systems: a data-driven approach, *IEEE Trans. Autom. Sci. Eng.*, **22** (2025), 21376–21386. https://doi.org/10.1109/TASE.2025.3610951

45. J. S. Zhao, X. Zhang, Z. Y. Sun, W. H. Zhang, Event-triggered-based adaptive neural network secure strategy for stochastic networked nonlinear systems under DoS attacks, *IEEE Trans. Autom. Sci. Eng.*, **22** (2025), 18920–18932. https://doi.org/10.1109/TASE.2025.3592216

46. L. X. Zhu, Y. Q. Wang, G. M. Zhuang, G. F. Song, Dynamic-memory event-based asynchronous dissipative filtering for T-S fuzzy singular semi-Markov jump systems against multi-cyber attacks, *Appl. Math. Comput.*, **431** (2022), 127352. https://doi.org/10.1016/j.amc.2022.127352

47. J. H. Yuan, W. Sun, Y. Sun, S. F. Su, Mask privacy preservation prescribed-time consensus control for nonlinear multi-agent systems, *IEEE Trans. Autom. Sci. Eng.*, **22** (2025), 11554–11563. https://doi.org/10.1109/TASE.2025.3535924

48. G. M. Zhuang, Y. J. Pang, G. D. Zong, J. W. Xia, NN-based dynamic adaptive triggered security compensation feedback control for implicit power systems subjected to FDI attacks, *IEEE Int. Things J.*, **12** (2025), 50493–50502. https://doi.org/10.1109/JIOT.2025.3609853

49. E. Jafari, T. Binazadeh, A novel event-triggered nonlinear control approach for descriptor systems with time-varying delay and input saturation constraints, *Eur. J. Control*, **86** (2025), 101384. https://doi.org/10.1016/j.ejcon.2025.101384

50. F. Amato, G. De Tommasi, S. Dubbioso, F. Fiorenza, D. G. Lui, Finite-time stability and stabilization for linear time-varying descriptor systems, *IFAC PapersOnLine*, **59** (2025), 61–66. https://doi.org/10.1016/j.ifacol.2025.09.525

51. G. M. Zhuang, Y. R. Fu, J. W. Xia, Y. Q. Wang, Estimator-based attack-tolerant compensation control for discrete singular systems under FDI attacks and hybrid IDVs-dependent event-triggered mechanism, *IEEE Trans. Autom. Sci. Eng.*, **22** (2025), 23620–23630. https://doi.org/10.1109/TASE.2025.3629330

52. W. Zhang, G. C. Pang, X. Y. Chen, X. J. Mou, J. L. Qiu, J. D. Cao, Projective group consensus fault-tolerant control for multi-agent systems under time-varying polynomial faults and input constraints, *Commun. Nonlinear Sci. Numer. Simul.*, **161** (2026), 110208. https://doi.org/10.1016/j.cnsns.2026.110208

53. Y. J. Zhao, G. C. Pang, X. Y. Chen, J. L. Qiu, J. D. Cao, Robust fault-tolerant control for switched systems based on adaptive unknown input observer, *Commun. Nonlinear Sci. Numer. Simul.*, **140** (2025), 108416. https://doi.org/10.1016/j.cnsns.2024.108416

54. Z. R. Cao, Y. Niu, J. Song, Finite-time sliding-mode control of Markovian jump cyber-physical systems against randomly occurring injection attacks, *IEEE Trans. Autom. Control*, **65** (2020), 1264–1271. https://doi.org/10.1109/TAC.2019.2926156



AIMS Press

© 2026 the Author(s), licensee AIMS Press. This is an open access article distributed under the terms of the Creative Commons Attribution License (https://creativecommons.org/licenses/by/4.0)